

# Using of Isolated Hydroxyapatite from Sheep Bones to Remove Lead (II) from Aqueous Solution and Studying the Thermodynamics and Adsorption Isotherm

Zaki N. Kadhim

Department of Chemistry, College of Science, University of Basrah  
(Basrah, IRAQ)  
Email: zekinasser99 [AT] yahoo.com

---

**ABSTRACT**— *In this paper, Cleaned sheep's bone pieces were heated at 1100°C to isolate hydroxyapatite(HAP). FTIR spectrometry and the X-ray diffractometry was confirmed the presence of HAP. Kinetic batch experiments were used to study the adsorption behavior of Pb<sup>2+</sup> in HAP. The isothermal models Langmuir, Freundlich, Temkin and Dubinin-Kaganer-Radushevich (DKR) were applied to describe the adsorption properties by investigation the contact time, lead concentration and temperature. The equilibrium uptake of lead ions by isolated hydroxyapatite was fitted with Langmuir isotherm model. Thermodynamic parameters free energy change ( $\Delta G^{\circ}$ ), enthalpy change ( $\Delta H^{\circ}$ ) and entropy change were also calculated for adsorption process of lead and the results indicated that the adsorption reaction were spontaneous( $\Delta G^{\circ} < 0$ ), endothermic ( $\Delta H^{\circ} > 0$ ) and pseudo first and second order both fitted the adsorption process of lead ions on isolated hydroxyapatite.*

**Keywords**— Hydroxyapatite, Adsorption Isotherm, Lead (II), Thermodynamics.

---

## 1. INTRODUCTION

Hydroxyapatite (HAP) belongs to the group of calcium phosphates, under which ceramic materials with different amounts of calcium and phosphorus are classified. The name apatite was described by the general chemical formula  $M_{10}(XO_4)_6Z_2$  where M could be  $Ca^{2+}$ ,  $Ba^{2+}$ ,  $Sr^{2+}$ ,  $Pb^{2+}$ ,  $Mg^{2+}$ ,  $Zn^{2+}$ ,  $Si^{2+}$  or  $Na^+$ ; X could be  $P^{5+}$ ,  $V^{5+}$ ,  $Cr^{5+}$  or  $Mn^{5+}$  and Z could be Cl, F or OH<sup>-</sup> [1].

The term “apatite” is derived from the Greek word “apatao” which means “to deceive”. Probably, the structural similarity of different possible mineral compositions was deceiving or misleading to ancient Greek researchers. HAP [ $Ca_{10}(PO_4)_6(OH)_2$ ] is the inorganic component of the natural bone and teeth, but it can be chemically synthesized [2,3]. It is an important material in biology and chemistry. HAP is normally used medically, where HAP and HAP containing polymer-ceramics are important components of the current and the future biomedical materials, also it has non-medical applications [4].

Although HAP manufacture is a standard practice in untied states of America, Europe and Japan, the cost of this material to non HAP manufacturing, country or countries with developing economies remains very high; therefore, requiring a cheaper local HAP source [5]. Given that bone account for about 16-20% of the carcass weight and the current worldwide drive to be more economically efficient in the processing of raw products, achieving added value other than meat uses, such as bone use, is an important priority [6]. Considerable efforts were invested into the study of the effect of the heat treatment on the bone, since the calcined bone can be used as osteoreproductive biomaterial for filling osteal defects [7].

Lead is very toxic element and it founds in trace quantities in environments. Lead toxicity can affect every organ system. On a molecular level, proposed mechanisms for toxicity involve fundamental biochemical processes. These include lead's ability to inhibit or mimic the actions of calcium and to interact with proteins [8]. The diagnosis of lead toxicity has conventionally been based on considerably elevated blood lead levels. However, information now indicates that low-level exposures resulting in blood lead levels lower 10  $\mu\text{g/dL}$  result in cognitive dysfunction, neurobehavioral disorders, neurological damage, hypertension, and renal impairment [9]. Thus, for the sake of ecosystem constancy and communal health, it is of enormous imminence to eliminate lead ions from the environments. The aim of this study was to investigate the adsorption behavior of lead (II) ions from aqueous solution. Adsorption conditions were studied. Adsorption mechanisms and isotherms were analyzed.

## 2. EXPERIMENTAL

### 2.1 Materials

All chemicals used in this study were of analytical grade and the aqueous solution were prepared using double distilled water.

### 2.2 Isolation of HAP

The hydroxyapatite was isolated as follow: Cattle shoulder bones were collected from local commercial butcheries in Basrah. The bone samples were thoroughly washed with distilled water to remove the macroscopic adherent impurities, and then cut into small pieces. The bone pieces were boiled in distilled water for 12 hours using hot plate (water changed every 2 hours) to avoid soot and crack formation during the heat treatment that would be achieved in next time by removing meat pieces, bulk surface fat and connective tissues. Then, the bone pieces were filtered using sieve and dried by vacuum oven. Later, the dry bone pieces were degreased by immersing in acetone-ether mixture at a ratio of 3:2 for 24 hours, and then, filtered and dried. The chemically treated bone pieces were heated using muffle furnace at 1100°C [10].

### 2.3 Characterization of HAP

The Fourier Transform Infrared Spectroscopy Analysis (FTIR-Shimadzu, 8400S) was carried out using KBr pellets. The analysis was carried out in the range between (4000 - 400)  $\text{cm}^{-1}$ . The X - ray diffraction analysis (XRD) of crystal phase of HAP was identified by powder X-ray diffraction using (X'pert pro MPD/PANalytical) with  $\text{CuK}\alpha$  (1.545 Å) radiation.

### 2.4 Sorption Experiment

A stock solution of  $\text{Pb}^{2+}$  of concentration 500mg/L was prepared by dissolving suitable quantity of  $\text{Pb}(\text{NO}_3)_2$  in deionized water. A lower concentrations of (100, 150, 200 and 250 mg/L) were prepared. The pH was adjusted to 5.5 by addition the drop wise of 0.1M NaOH or 0.1 M  $\text{HNO}_3$ . Batch adsorption procedures were carried out in aqueous solution by mixing 0.1 g HAP with 100- 250mg/L  $\text{Pb}^{2+}$  solution in 500 mL conical flask. The time interval of 5 to 120 minutes was used to determine the equilibrium time. The sample solution is shaken 10 min at 250 rpm and 30 °C. The concentration of the metal ions are analyzed by using atomic adsorption spectrophotometer. The procedure was carried out in duplicate and the mean value was calculated to minimize the errors. The Adsorption removal capacity of the HAP for metal ions was calculated using equation (1).

$$q_e = \frac{V(C_0 - C_e)}{m} \dots \dots \dots (1)$$

Where  $C_0$  and  $C_e$  (mg/L) are the initial and equilibrium  $\text{Pb}^{2+}$  concentrations, respectively, V(L) is the volume of the solution and m is the mass of the adsorbent.

The percent removal (%) and distribution ratio ( $K_d$ ) were calculated using equation (2 and 3).

$$\% \text{Removal} = \frac{(C_{i0} - C_f)}{C_{i0}} \times 100 \dots \dots \dots (2)$$

Where  $C_0$  and  $C_f$  are the concentrations of  $\text{Pb}^{2+}$  ion in initial and final solution after equilibrium time respectively.

$$K_d = \frac{\text{amount of metal in adsorbent}}{\text{amount of metal in solution}} \times \frac{V}{m} \dots \dots \dots (3)$$

Where V is the volume of the solution (mL) and m is the mass of the adsorbent (g).

## 3. RESULTS AND DISCUSSION

### 3.1 Characteristics of HAP

The structure of isolated HAP was identified using FTIR spectroscopy as shown in Fig.(1). The spectrum indicate the presence of  $\text{PO}_4^{3-}$  and  $\text{OH}^{-1}$  ion in all of these samples. The bands at 1035-1045  $\text{cm}^{-1}$  and 970-960  $\text{cm}^{-1}$  were assigned to the stretching vibration of P=O, while 605  $\text{cm}^{-1}$  and 568  $\text{cm}^{-1}$  were assigned to its deformation mode [11]. Bands at 3570  $\text{cm}^{-1}$  and 634  $\text{cm}^{-1}$  were assigned to the vibration motion of the  $\text{OH}^{-1}$  ions [12].

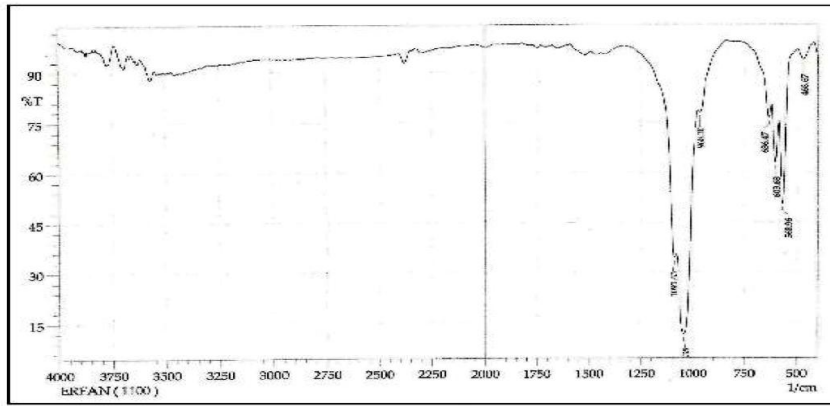


**Figure 1:** FTIR Spectrum of Isolated HAP.

The X-ray diffraction considered as a finger print for the compound. The most important parameter in the confirmation of the structure of a compound is the  $d$  value, which represents the distance between atomic planes in a crystal. The  $d$  values must be consistent for any diffractogram of the same compound. The allowed difference in the  $2\theta$  values among the diffractograms of the same compound is 0.3 [13]. The X-ray diffraction pattern of the powdered form of the bone sample heated at 1100°C is shown in Fig.(2). The observed positions of the diffraction lines ( $2\theta$  and corresponding  $d_{2\theta}$ ) and their relative intensities ( $I_{rel}$ ) are listed in Table (1). The  $d_{2\theta}$  values were calculated according to an equation derives from Bragg law [14]. This is stated below in equation (4) :

$$d (nm) = 0.154 \sqrt{2} \sin \theta \dots \dots \dots (4)$$

Where  $\theta$  represents the angle between the incident X-ray beam and crystal surface layers planes. The relative intensities of the diffraction lines were determined as diffraction line heights relative to the most intense line normalized to the intensity of 100. The  $d_{2\theta}$  and  $I_{rel}$  values obtained for the bone sample heated at 1200 °C are almost at full agreement with corresponding reference values reported for HAP [3]. These results confirm the formation of HAP.

**Table 1:**  $2\theta$  values,  $d_{2\theta}$  values,  $I_{rel}$  values observed for bon sample heated at 1200°C with the  $d_{reference}$  values.

Sequence	$2\theta$	$d_{2\theta}$ (nm)	$d_{reference}$ (nm)	$I_{rel}$
1	25.9	0.343	0.344	26
2	28.25	0.315	0.317	8
3	29	0.307	0.308	18
4	31.85	0.280	0.281	100
5	32.2	0.277	0.278	48
67	33	0.271	0.272	72
8	34.15	0.262	0.263	20
9	35.5	0.252	0.253	6
10	39.3	0.2289	0.2297	8
11	40.1	0.2245	0.2263	32
12	42.1	0.2143	0.2150	8
13	44.1	0.2051	0.2063	6
14	45.4	0.1995	0.2000	8
15	47	0.1931	0.1944	43
16	48.2	0.1885	0.1891	13
17	49.6	0.1835	0.1841	34
18	50.65	0.1800	0.1807	20

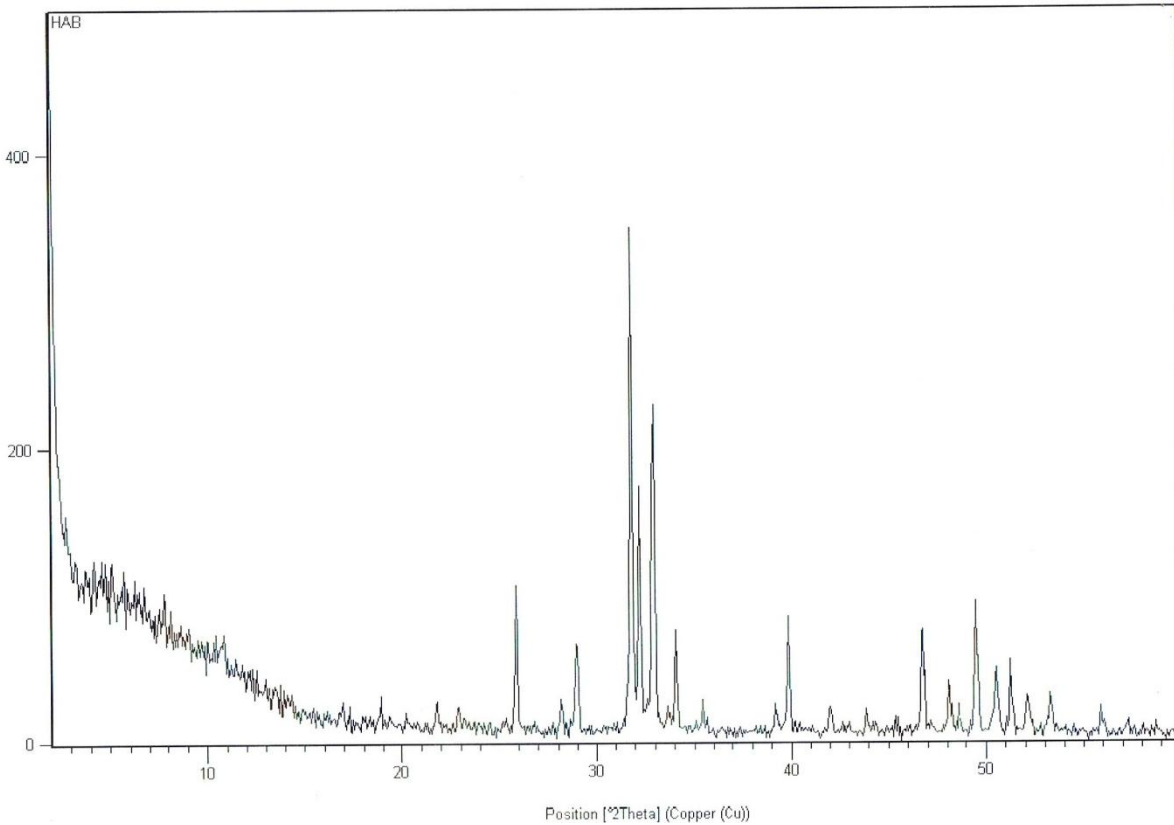


Figure 2: X-ray diffraction (XRD) pattern of Isolated HAP.

### 3.2 Effect of Lead (II) Concentration

The studies of effect of lead ions adsorption by HAP were carried out in range of 100-250mg/L. The Adsorption of the heavy metal ions was quite fast at the beginning suggesting surface reaction take place [15]. As shown in Fig.(3),when the initial of lead (II) concentration increased from 100 to 250 mg/L, the uptake capacity of HAP increase from 74 to 212 mg/g. The increase in adsorption capacity of HAP with an increase in initial  $Pb^{2+}$  ions concentration is a consequence in driving force due to concentration gradient arises between the bulk solution and surface of HAP. At higher concentration of  $Pb^{2+}$  ions, the active site of HAP were surrounded by much more metal ions and HAP surface was no more available to metal ions. As the process of adsorption continues, leading to less uptake of metal ions from the solution by HAP.

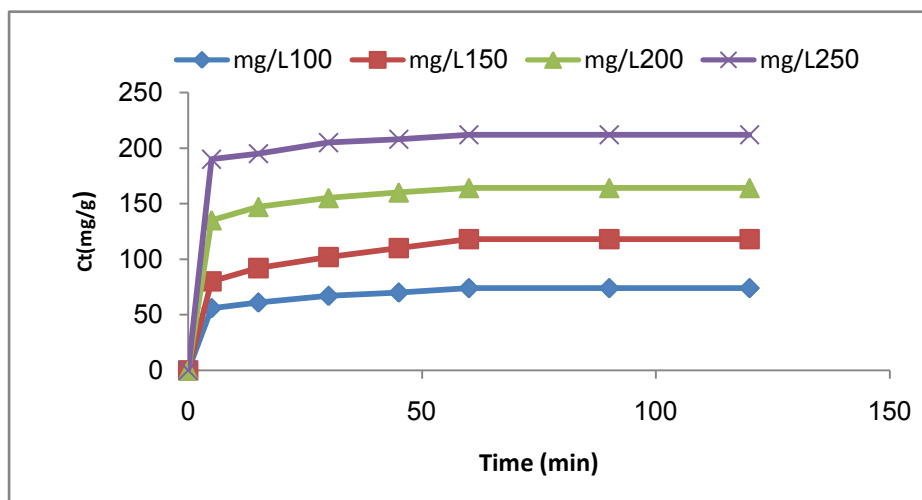


Figure 3: Time dependent Concentration on removal of  $Pb^{2+}$ .

Removal of the lead (II) ions by HAP with time in variety metal ions concentration is shown in Fig.(4), the removal process has been took place in two steps. Firstly, lead was removed fast but the in second step it was take place slowly and exhibited a later removal until equilibrium was reached. The major reason for the manifestation of the fast step is the abundance active sites on the HAP at the first period of adsorption process and ongoing residence of these sites causes to emerging of lower step[16].

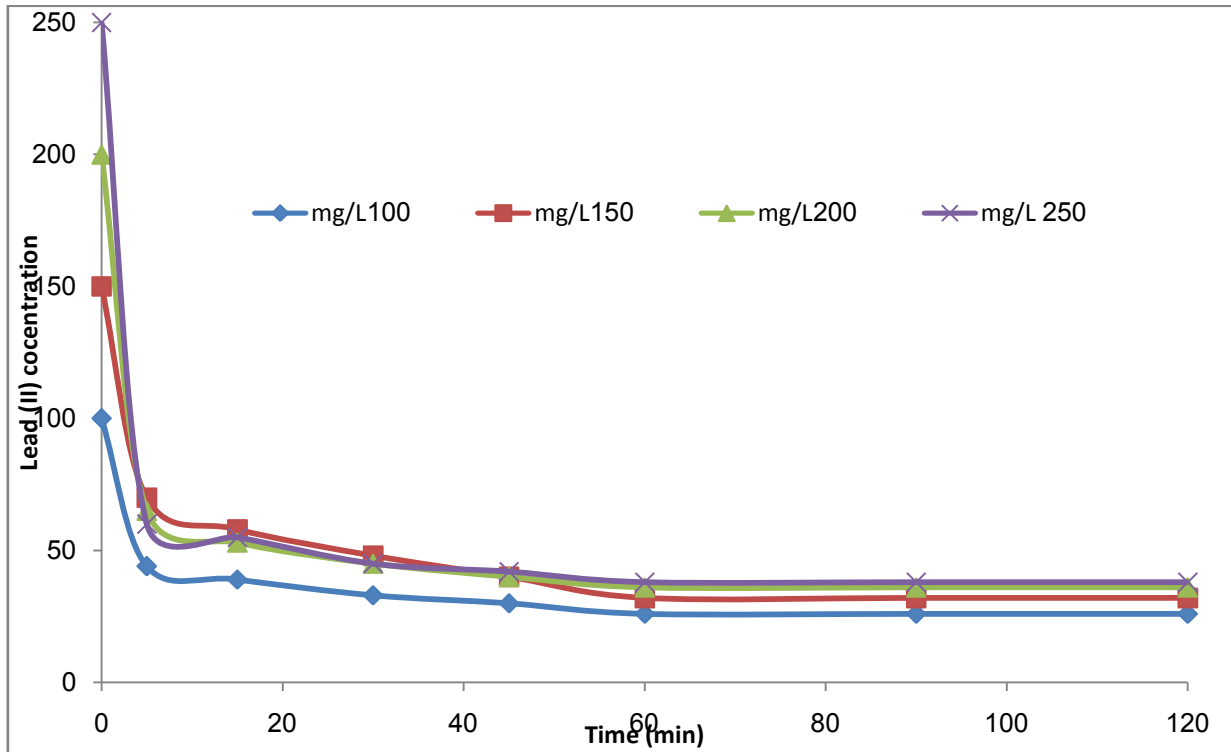


Figure 4: Effect of initial concentration of  $Pb^{2+}$  in different contact time.

### 3.3 Effect of Temperature

The temperature of reaction is the most important parameters as it enhances the movement of ions. Adsorption experiments achieved at four different temperatures (303, 313, 323 and 333 K) with 100mg/L Lead (II) concentration. The results are shown in Fig.5, these results show that high temperature is beneficial for removal the  $Pb^{2+}$  ion on HAP. The lead ions exist in water have hydration scabbard around there, that need to removed for direct interaction of lead ions with HAP surface. The raising of temperature my cause more cations attain sufficient energy to interact with HAP surface, hence, adsorption if preferable at high temperature [17].

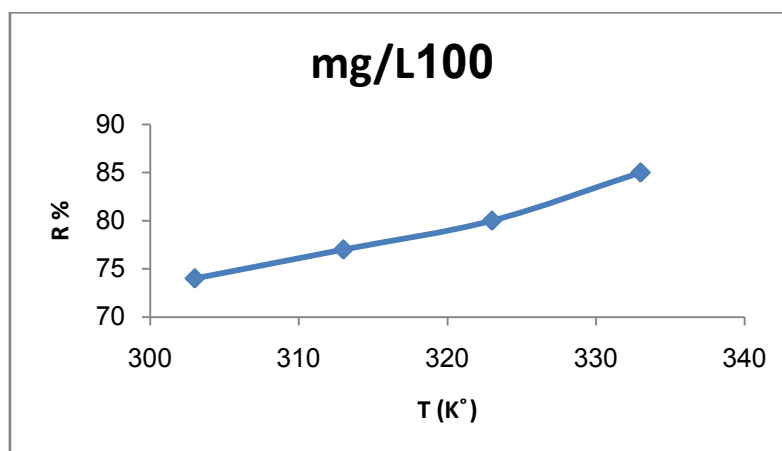


Figure 5: The removal capacity of lead (II) at different temperatures.

**3.4 Thermodynamic Functions**

Thermodynamic parameters such as free energy change ( $\Delta G^\circ$ ), enthalpy change ( $\Delta H^\circ$ ) and entropy change ( $\Delta S^\circ$ ) were deduced by means of the dependence of distribution coefficient  $K_d$  on temperature. The values of  $K_d$  were calculated at different temperature (Table 2). The entropy  $\Delta S^\circ$  and enthalpy  $\Delta H^\circ$  changes were determined as 70.818 J/mol. K and 18944 J/mol., respectively from  $\Delta G^\circ$  versus temperature plot (Fig. 6) that given by the following equation [18]:

$$\Delta G^\circ = -RT \ln K_d \dots\dots\dots(5)$$

Where  $\Delta G^\circ$  is standard free energy in (J), R is the ideal gas constant ( $8.314 \text{ J mol}^{-1} \text{ K}^{-1}$ ) and T is the absolute temperature (K).

Enthalpy change ( $\Delta H^\circ$ ) and entropy change ( $\Delta S^\circ$ ) were calculated from equation (6).

$$\Delta G^\circ = \Delta H^\circ - T \Delta S^\circ \dots\dots\dots(6)$$

**Table 2:** Thermodynamics parameter for adsorption  $\text{Pb}^{2+}$  on HAP.

Temp.K <sup>0</sup>	K <sub>d</sub>	$\Delta G^\circ$ (J/mol.)	$\Delta H^\circ$ (J/mol.)	$\Delta S^\circ$ (J/mol.K <sup>0</sup> )
303	2.846	-2635	18944	70.818
313	3.347	-3144		
323	4	-3723		
333	5.666	-4802		

According to Fig. 6 positive value of  $\Delta H^\circ$  propose endothermic behavior of adsorption and negative value of  $\Delta G^\circ$  signify the spontaneous behavior of the adsorption process. However, the negative value of  $\Delta G^\circ$  was found to diminish with increasing in temperature, signifying that spontaneous behavior of adsorption is inversely proportional to the temperature. The positive value of  $\Delta S^\circ$  show increased randomness at the solid/ solution interface during the adsorption.

**3.5 Adsorption isotherms**

The data analysis of sorption equilibrium isotherms are important for propose adsorption system. It is described by definite constants that values states the surface and attraction of the adsorbent that can be used to estimate the adsorptive capacity at equilibrium. The adsorption data can be studies by diverse adsorption isotherms such as Langmuir[19], Freundlich [20], Temkin [21] and Dubinin-Kaganer-Radushevich (DKR) [22].

The Langmuir isotherm model has been extensively used in adsorption studies. It describes the deposition of adsorbate species on the free surface of the adsorbent and formation of a monolayer adsorbate on the outer surface of adsorbent and can be represented as:

$$\frac{C_e}{q_e} = \frac{1}{Q_0 K_L} + \frac{C_e}{Q_0} \dots\dots\dots(7)$$

Where  $C_e$  is the equilibrium concentration of metal in solution (mg/L),  $q_e$  is the amount absorbed at equilibrium onto HAP (mg/g),  $Q_0$  and  $K_L$  are Langmuir constant related to adsorption capacity and adsorption energy, respectively. ( $Q_0$ ) represents the maximum adsorption capacity of monolayer coverage of adsorbent with adsorbate and  $K_L$  represents enthalpy of adsorption and should vary with temperature. The values of  $Q_0$  and  $K_L$  are computed by plot is obtained when  $C_e/q_e$  is plotted against  $C_e$  (Fig. 6), the constants  $Q_0$  and  $K_L$  were obtained from the slope and intercept, respectively. The Langmuir isotherm parameters are listed in Table (3). The important features of Langmuir model may be states in terms of dimensionless constant  $R_L$  known as separation factor given in equation (8):

$$R_L = \frac{1}{1 + K_L C_e} \dots\dots\dots(8)$$

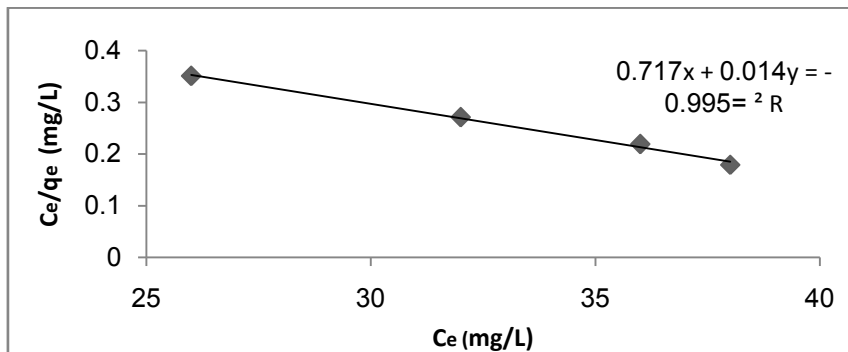


**Figure 6:**Langmuir adsorption isotherm of lead (II).

The plotting of values of separation factor  $R_L$  against the initial concentration  $C_o$  (mg/L) as shown in Fig. (7). The values of  $R_L$  lies in the rang  $0 < R_L < 1$  indicating that adsorption of lead ions on surface HAP is favorable. In addition, the adsorption is favorable at both low and high initial concentration as the values of  $R_L$  are very close to zero.

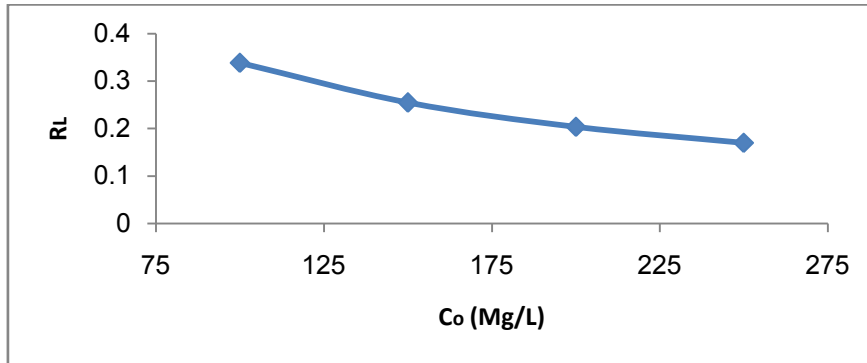


**Figure 7:**  $R_L$  values based on Langmuir isotherm.

The Freundlich isotherm models is empirical equations assumes that the removal of metal ions happen on a heterogeneous adsorbent surface. This model is considered to be suitable for describing the multilayer adsorption. This model was applied in order to determine the removal capacity of lead (II) ions. The linear Freundlich isotherm equation is:

$$\log q_e = \ln K_f + \frac{1}{n} \log C_e \dots \dots \dots (9)$$

Where  $q_e$  (mg/g) is the amount of metal ion adsorbed on adsorbent at equilibrium,  $C_e$  (mg/L) the equilibrium concentration of metal ion in the solution,  $K_f$  (L/g) is a constant describing the adsorption capacity and  $n$  is empirical parameter related to the adsorption intensity. The plot of  $\log q_e$  against  $\log C_e$  is shown in Fig.(8),  $K_f$  and  $n$  were obtained from the slope and intercept, respectively. When  $1/n$  values are in range  $0.1 < 1/n < 1$ , the adsorption process is desirable. The Freundlich isotherm parameters are listed in Table (3).

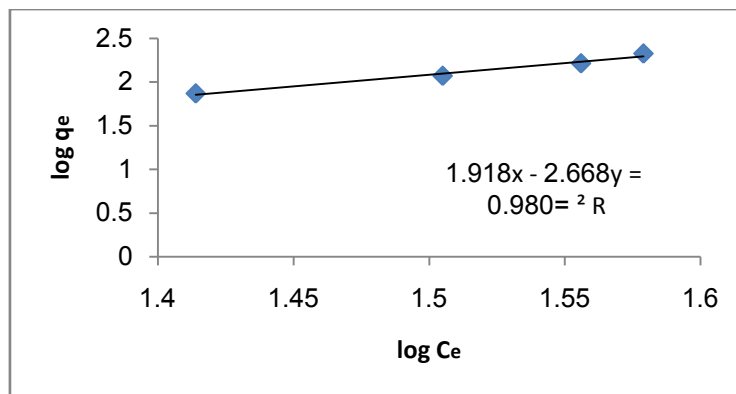


**Figure 8:** Freundlich isotherm model.

Temkin isotherm models, contrary to the Langmuir and Freundlich isotherms, this model take into account the interactions between adsorbents and metal ions to be adsorbed and is based on the adsorption that the free energy of adsorption is simply a function of surface coverage. Temkin linear form represented by the following expressions:

$$q_e = \frac{RT}{b_T} \ln A_T + \frac{RT}{b_T} \ln C_e \dots \dots \dots (10)$$

Where  $[RT/b_T]$  in (J/mol.) corresponding to the heat of adsorption,  $R$  is ideal gas constant,  $T$ (K) is the absolute temperature,  $b_T$  is the Temkin isotherm constant and  $A_T$  (L/g) is the Temkin equilibrium binding constant corresponding to the maximum binding energy. The linear plot of Temkin isotherm model at 303 K, the constants  $b_T$  and  $A_T$  are determined from the slope and intercept of the plot shown in Fig. (9). The Tamkin model parameters are presented in Table (3).

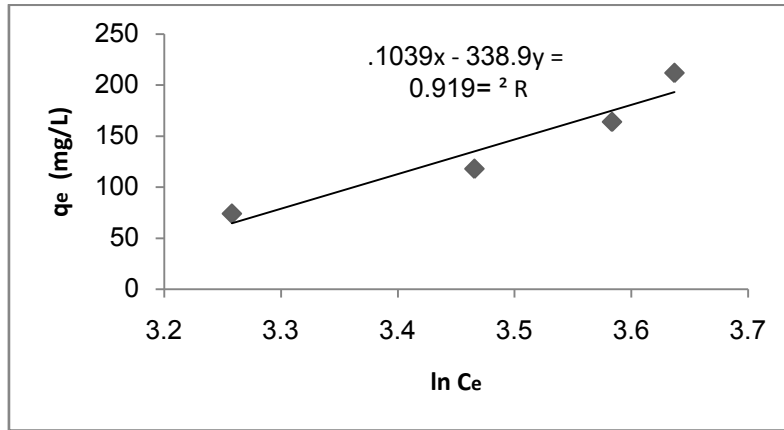


**Figure 9:** Temkin adsorption isotherm of lead (II) ions.

The Dubinin-Kaganer-Radushkevich (DKR) isotherm has been used to represent the adsorption of metal ions on HAP. In the equation cited below:

$$\ln C_{ads} = \ln X_s - K_{ad} \varepsilon^2 \dots \dots \dots (11)$$

Where  $C_{ads}$  (mol/g) is the number of metal ions adsorbed per unit weight of adsorbent.  $X_s$  (mol/g) is the maximum sorption capacity,  $K_{ads}$  ( $\text{mol}^2/\text{J}^2$ ) is the activity coefficient related to mean sorption energy and  $\varepsilon$  is DKR isotherm constant can be calculated as:

$$\varepsilon = RT \ln \left[ 1 + \frac{1}{C_0} \right] \dots \dots \dots (12)$$

Where  $R$  is the ideal gas constant and  $T$  is the absolute temperature (K). The saturation capacity  $X_s$  describes the total specific micropore volume of the sorbent. The DKR model was generally applied to differentiate the physical and chemical adsorption ions through its mean free energy,  $E$  per molecule of adsorbate. The sorption energy can be calculated by the following relationship:

$$E = \left[ \frac{1}{\sqrt{2K_{ads}}} \right] \dots \dots \dots (13)$$

The plot of  $\ln C_{ads}$  vs  $\varepsilon^2$  was shown in Fig.(10). Type of adsorption could be predictable by calculation of observable adsorption energy. If  $E$  value lower than 8 kJ/mol, the adsorption form can be construed by physical adsorption, if  $E$  value (8-16 kJ/mol.) the adsorption form can be construed by ion exchange, if  $E$  larger than 16 kJ/mol. the adsorption can be explained by stronger chemical adsorption. The Dubinin-Kaganer-Radushkevich (DKR) isotherm parameters are listed in Table (3).

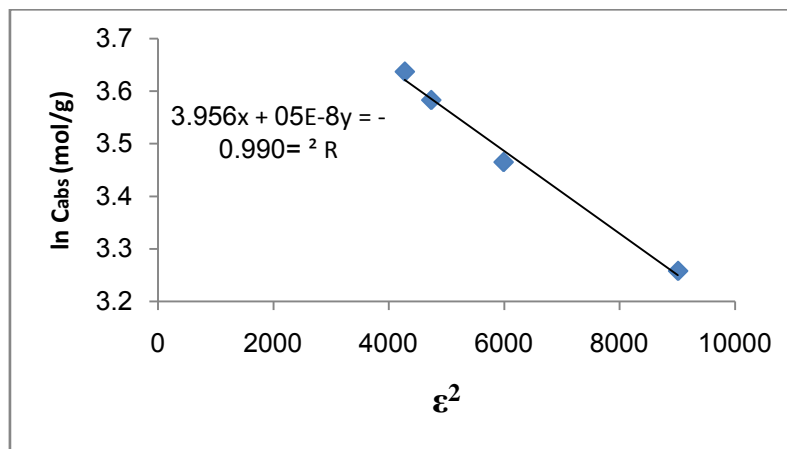


**Figure 10:** The Dubinin-Kaganer-Radushkevich isotherm of lead (II) ions

**Table 3:** Isotherm parameters for Langmuir , Freundlich, Temkin and DKR models.

Type of Isotherm	Parameters	Value
<b>Langmuir</b>	$Q_0$	71.428 (mg/g)
	$K_L$	0.01952
	$R_L$	0.3386
	$R^2$	0.9952
<b>Freundlich</b>	$K_f$	82.927 (L/g)
	$1/n$	2.668
	$n$	0.374
	$R^2$	0.9807
<b>Temkin</b>	$b_T$	7.443
	$A_T$	21.47 (L/mg)
	$R^2$	0.9192
<b>DKR</b>	$K_{ad}$	$8 \times 10^{-5}$ (mol. <sup>2</sup> /kJ <sup>2</sup> )
	$X_s$	52.2948 (mol./g)
	$E$	7.07 (kJ/mol)
	$R^2$	0.9905

The aggregation factors R (0.9952,0.9807, 0.9192 and 0.9905) for Langmuir , Freundlich, Temkin and DKR models, respectively, emphasize a good conformity between both theoretical and experimental data. The values listed in Table (3) signified that the adsorption pattern that the Langmuir isotherm has the excellent fitted for the desorption of lead (II) ions on isolated HAP.

**3.6 Adsorption Kinetics**

In order to examine the mechanism of adsorption, the pseudo-first order kinetic and pseudo-second order kinetic model were studied. They kinetic studies were achieved by using the linear form of pseudo first order and pseudo second order equations that given by [23,24] :

$$\log(q_e - q_t) = \log q_e - \frac{K_1}{2.303} t \dots \dots \dots (14)$$

$$\frac{t}{q_t} = \frac{1}{K_2 q_e^2} + \frac{t}{q_e} \dots \dots \dots (15)$$

Where  $q_e$  and  $q_t$  (mg/g) are metal ion adsorption capacities for adsorbent at equilibrium and at time  $t$ , respectively,  $K_1$  and  $K_2$  ( $g \text{ min}^{-1} \text{ mg}^{-1}$ ) are represent the equilibrium rate of first and second order adsorption respectively. The parameters  $K_1$  and  $q_e$  were directly obtained from the intercept and slope of the plot of  $\log(q_e - q_t)$  versus  $t$  of which the plotted results are shown in Fig. (11). By plotting  $t/q_t$  against  $t$  shown in Fig. (12). The second order constant  $K_2$  and  $q_e$  were obtained from intercept and slope of curve. The parameters obtained from the curves are listed in Table 4.

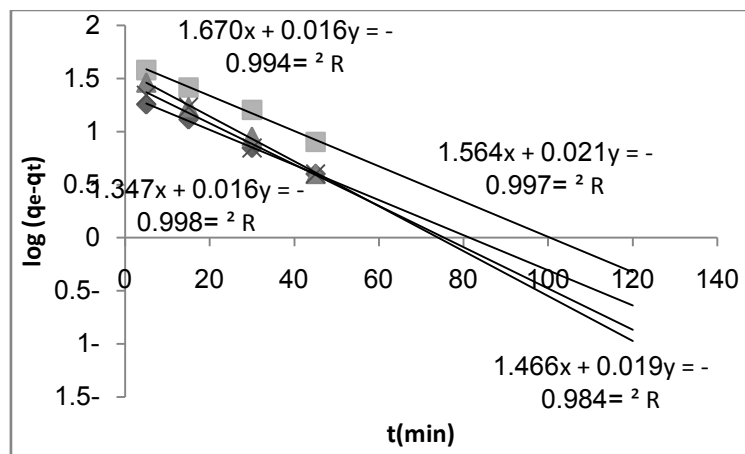


**Figure 11:** Adsorption Kinetic of pseudo first order kinetic of Lead(II).

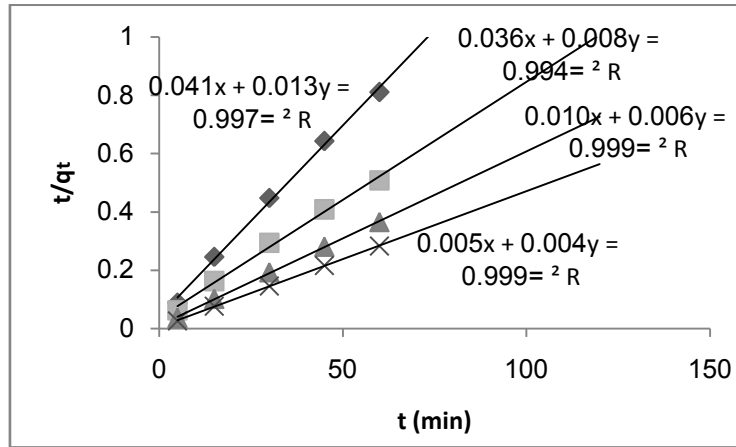


Figure 12: Adsorption Kinetic of pseudo-second order of Lead(II).

Excellent agreement exists between the model and the experimental results for both the pseudo first ( $R^2 = 0.9986, 0.9941, 0.9976$  and  $0.9848$ ) and pseudo second order ( $R^2 = 0.9971, 0.9945, 0.9994$  and  $0.9997$ ). The same kinetic model was used to describe the sorption kinetic of metal ions on isolated HAP.

Table 4: Kinetic parameters of Lead (II) on HAP.

Pseudo-first order			Pseudo-second order			
$q_{e1}(\text{mg/g})$	$K_1 \text{ min}^{-1}$	$R^2$	$q_{e2}$	$K_2 (\text{g/mg min})$	$R^2$	$q_{\text{exp}}$
22.240	0.0382	0.9986	76.330	0.0041	0.9971	74
46.830	0.0382	0.9941	123.456	0.0018	0.9945	118
36.670	0.0486	0.9976	166.600	0.0033	0.9994	164
29.290	0.0446	0.9848	212.760	0.0041	0.9997	212

The calculated  $q_{e2}$  values were predictable from pseudo second order model and were found to be consistent with experimental ones. The calculated  $q_{e1}$  values obtained from pseudo first order plot were found to be different with experimental values.

The intraparticle diffusion model [25] can be express as follows:

$$q_t = K_d t^{1/2} + C \dots \dots \dots (16)$$

Where  $K_d (\text{mg/g min}^{1/2})$  is the intraparticle diffusion rate constant and C is constant. The relationship between  $q_t$  and  $t^{1/2}$  at different concentration did not found to initiate from zero (fig., signifying that intraparticle diffusion step subjugated the adsorption process before equilibrium accomplished. Because of the intraparticle diffusion was not found to be rate determining step therefore, intraparticle diffusion model is not appropriate for  $\text{Pb}^{2+}$  adsorption by isolated HAP.

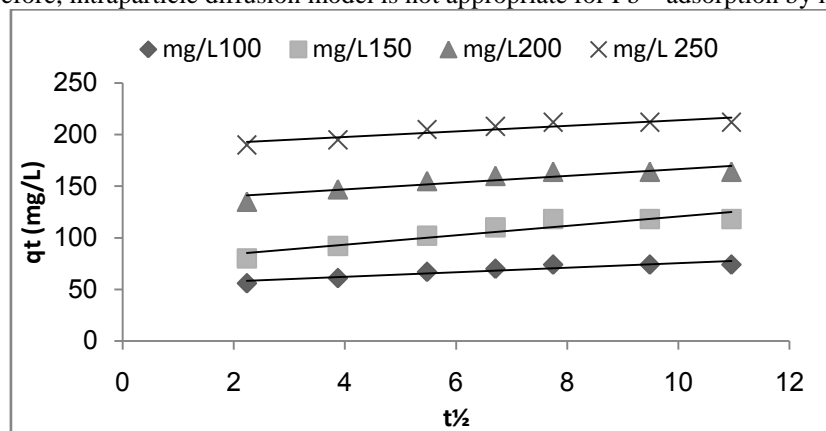
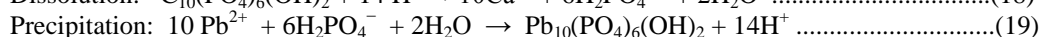
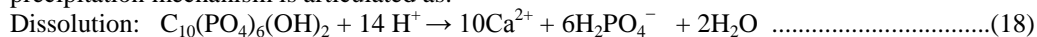


Figure 13: Intraparticle diffusion kinetic of  $\text{Pb}^{2+}$  on HAP.

There are many types of reactions competent of up taking lead ions from solution. The first reaction is the adsorption of  $Pb^{2+}$  on the surfaces followed by the ion exchange reaction between lead ions adsorbed and calcium ions of HAP ( $Ca_{10}(PO_4)_6(OH)_2$ ). The ion exchange interaction can be done as follows:



The other reaction is dissolution of HAP in aqueous solution surrounded by  $Pb^{2+}$  ions then the precipitation of lead apatite ( $Zn_{10}(PO_4)_6(OH)_2$ ). The presence of lead (II) ions and low pH were speed up hydroxyapatite dissolution, liberalized the  $PO_4^{3-}$  ions come together with  $Pb^{2+}$  ions to form the less soluble Pb-hydroxyapatite. The dissolution/precipitation mechanism is articulated as:



#### 4. CONCLUSION

The objective of this work to evaluate the influence of the isolated hydroxyapatite (HAP) to remove the lead ions from solution. The parameters effecting the adsorption process such as temperature and initial concentration of metal ions were examined. The removal process of lead ions by isolated HAP fitted with Langmuir adsorption isotherm model. Increasing the initial concentration leads to increasing the removal capacity of HAP. The maximum capacities of removal lead ions depends on temperature. The thermodynamic parameters  $\Delta G^\circ$ ,  $\Delta H^\circ$  and  $\Delta S^\circ$  were estimated. The negative value of  $\Delta G^\circ$  show the spontaneous behavior of adsorption process. The positive value of  $\Delta H^\circ$  indicated the endothermic behavior of adsorption process. The obtained results were exemplified that adsorption follow both the pseudo first order and pseudo second order kinetics.

#### 5. REFERENCES

- [1] Shalaby S.W., Salz U., "Polymers for Dental and Orthopedics Applications" Ch.3, pp. 79-80, CRC press ,Boca Raton.2007.
- [2] Chakraborty S., Bag S., Pal S., Mukherjee A.K., structural and microstructural characterization of bioapatite using X-ray powder diffraction and Fourier transform infrared technique *J. Appl. Cryst.*, vol. 39, pp.385-390, 2006.
- [3] Markovic M., Fowler B.O., Tung M.S., Preparation and Comprehensive Characterization of a Calcium Hydroxyapatite Reference Material, *J. Res. Natl. Inst. Technol.*, vol.109, pp.553-568, 2004.
- [4] - Morales J.G., Burgues J.T., Fraile T.B., Clemente R.R., Precipitation of Stoichiometric Hydroxyapatite by a Continuous Method *Cryst. Res. Technol.*, vol.36, pp.15-26, 2001.
- [5] Mucalo M.R., Foster D.L., Wielage B., Steinhäuser S., Mucha H., Knichton D., Kirby J., *J. Appl. Biomater. Biomech*, vol.2, pp.96-104,2004.
- [6] Mucalo M.R., Foster D.L., A method for Avoiding the Xanthoproteic-associated Discolouration in Reprecipitated (Nitric-acid-digested) Hydroxyapatite Prepared from Mammalian Bone Tissue, *Croat. Chem. Acta.*, vol.77, pp.509-517, 2004.
- [7] Danilchenko S.N., Koropov A.V., Protsenko I.Y., Cleff B.S., Sukhadob L.F., Thermal behavior of biogenic apatite crystals in bone: An X-ray diffraction study. *Cryst. Res. Technol.*, vol.41, pp.268-275, 2006.
- [8] Needleman H.L., Bone lead levels in adjudicated delinquents: A case control study. *Neurotox. Teratol.*, vol.24, pp.711-717, 2002.
- [9] Patrick L., Lead Toxicity, A Review of the Literature. Part I: Exposure, Evaluation, and Treatment, *Altern. Med. Review*, vol.1, no.1, pp.1-22, 2006.
- [10] Ooi C.Y., Hamdi M., Ramesh S., Properties of hydroxyapatite produced by annealing of bovine bone. *Ceram. Inter.*, vol.33, 1171-1177, 2007.
- [11] Featherstone J.D., Pearson S., Geros R.Z., An infrared method for quantification of carbonate in carbonated apatites, *Caries Res.*, vol.18, pp.63-66, 1984.
- [12] Rogers K.D., Daniels P., An X-ray diffraction study of the effects of heat treatment on bone mineral microstructure, *Biomaterials*, vol.23, pp. 2577-2585,2003.
- [13] Wien T., "Measurement and Acquisition of X-Ray Diffractometry Spectra", Ch. 9, pp. 748-752, Warsaw, 1995.
- [14] Pardo B., Megademini T., André J.M., X-UV Synthetic Interference Mirrors : Theoretical Approach ,*Revue. Phys. Appl.* vol.23, pp. 1579-1597, 1988.
- [15] Zamani Z., Salahi E., Mobaserpour I., Removal of Nickel from Aqueous Solution by Nano- Hydroxyapatite Originated from Persian Gulf Corals. *Canadian Chemical Transactions*, Vol.1, no.3, pp.173-190,2013.
- [16] Shukla S.S., Yu, L.J. Dorris, K.L. Shukla A., Removal of Nickel from Aqueous Solution by sawdust, *J.Hazard. Mater.*, Vol.121, pp.243-246,2005.

- [17] Doan, H.D. Wu, J. Mitzakov R., Combined electrochemical and biological treatment of industrial wastewater using porous electrodes, *J. Chem. Technol. Biotechnol.*, vol.81, pp. 1398-1408, 2006.
- [18] Layla B A., Al-Najar A.A., Kadhim Z. N., Adsorption and Desorption Characteristics of Bispyribac-Sodium Pesticide in Eight Soil south of Iraq, *Inter, J. Sci. Eng. Rese.* vol.6, no7, pp. 1689-1700, 2015.
- [19] Langmuir I., The adsorption of gases on plane surface of glass, mica and platinum, *J. Am.Chem.Soc.*, vol.40, no.9, pp.1361-1403, 1918.
- [20] Freundlich H.M.F., Uber die adsorption in losungen, (Over the adsorption in solution) *Z.Phys.Chem.*, vol.57, pp.385-470, 1906.
- [21] Temkin M.I., Pyzhev V., Kinetics of ammonia synthesis on promoted iron catalyst, *Acta Phys. Chim., USSR* vo.12, pp.327-356, 1940.
- [22] Dubinin M.M., Zaverina E.D., Radushkevich L.V., Sorption and structure of active carbons, *J. Phy. Chem.*, vol.21, pp. 1351-1362, 1947.
- [23] Lagergren S., Zur theorie der sogenannten adsorption geloster stoffe, *Kunglia Svenska Vetenskapsakad, Handl*, vol.24, pp.1-39, 1898.
- [24] Ho. Y.S., McKay G., pseudo-second order model for sorption processes, *Biochem.* vol.34, pp.451-465, 1999.
- [25] Meski S., Ziani S., Khireddine H., Bouboub S. Zaidi S., Factorial design analysis for sorption of zinc on hydroxyapatite, *J. Hazard. Mater.* vol. 186, 1007-1017, 2011.
- [26] Valsami-Jones E., Rangarsdottir K.V., Putnis A., Basbach D., Kemp A.J., Cressey G., The dissolution of apatite in the presence of aqueous metal cations at pH 2-7, *Chem. Geol.* vol 151, pp. 215- 233, 1998.